

# Kinetic Analysis of the Photoinitiated Autocatalytic Chain Decomposition of Phenyl Azide. A Molecular Explosion in Solution

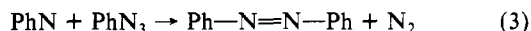
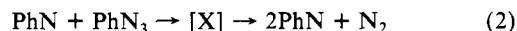
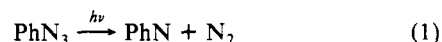
Joseph P. Costantino, Helen W. Richter, Celia H. Lee Go, and Walter H. Waddell\*

Contribution from the Department of Chemistry and Center for the Joining of Materials, Carnegie-Mellon University, Pittsburgh, Pennsylvania 15213. Received July 11, 1984

**Abstract:** Quantum yields of disappearance of phenyl azide [ $\phi(-\text{PhN}_3)$ ] were determined for oxygen-purged, oxygen-saturated, and air-saturated solutions in acetonitrile ranging in concentration ( $[\text{PhN}_3]$ ) from  $1.40 \times 10^{-5}$  to  $7.93 \times 10^{-1}$  M. A kinetic analysis of a simplified four-step reaction mechanism, based upon the reaction of phenylnitrene and phenyl azide to form two phenylnitrenes, affords a mathematical expression that relates experimentally determined  $\phi(-\text{PhN}_3)$  values to experimentally measured  $[\text{PhN}_3]$ ,  $I_0$  (intensity of the excitation light), and  $V_0$  (volume of solution irradiated) values. One general expression accurately fits 56 experimental determinations of  $\phi(-\text{PhN}_3)$ , correctly relating it to  $[\text{PhN}_3]$  and  $I_0$ , whereby  $\phi(-\text{PhN}_3)$  increases with increasing  $[\text{PhN}_3]^2$  and decreases with increasing  $I_0$ . The  $\phi(-\text{PhN}_3)$  data along with the kinetic analysis provide definitive evidence of the first molecular explosion in solution as a result of the photoinitiated autocatalytic (branching) chain decomposition reaction of phenyl azide.

Upon irradiation of dilute solutions of phenyl azide ( $\text{PhN}_3$ ) with ultraviolet light, molecular nitrogen is lost and phenylnitrene ( $\text{PhN}$ ) is formed,<sup>1-3</sup> eq 1. The quantum yield of the loss of molecular nitrogen ( $\phi(-\text{N}_2)$ )<sup>4-6</sup> and the quantum yield of disappearance of phenyl azide ( $\phi(-\text{PhN}_3)$ )<sup>7,8</sup> are essentially identical.  $\phi(-\text{N}_2)$  values of 0.52<sup>6</sup> and 0.43<sup>4,5</sup> are obtained upon irradiation of phenyl azide in nonpolar and polar solvents, respectively. A  $\phi(-\text{PhN}_3)$  value of ca. 0.5 is obtained upon irradiation of ca.  $2 \times 10^{-5}$  M phenyl azide in deoxygenated acetonitrile.<sup>7,8</sup> However, at higher phenyl azide concentrations ( $[\text{PhN}_3]$ ), the measured  $\phi(-\text{PhN}_3)$  values greatly exceed unit efficiency. Indeed,  $\phi(-\text{PhN}_3)$  values of approximately four thousand have been determined for  $[\text{PhN}_3] > 10^{-1}$  M.<sup>8</sup> Intermediate  $[\text{PhN}_3]$  affords  $\phi(-\text{PhN}_3)$  values between those of the  $10^{-5}$  and  $10^{-1}$  M solutions. However, the observed increase in  $\phi(-\text{PhN}_3)$  with increasing  $[\text{PhN}_3]$  is not a linear relationship, but it appeared to follow an exponential function.<sup>8</sup> In order to account for this concentration/reactivity behavior an autocatalytic, branching chain mechanism<sup>9</sup> was proposed which would require only 13 cycles to afford the observed  $\phi(-\text{PhN}_3)$  values at  $[\text{PhN}_3] > 10^{-1}$  M.<sup>8</sup> This photoinitiated autocatalytic chain decomposition (PACD) of phenyl azide is based on a photochemical initiation of the reaction (eq 1), branching chain propagation steps whereby phenylnitrene reacts with phenyl azide to afford two phenylnitrenes, whether or not a second intermediate (X) is involved<sup>10</sup> (eq 2), and chain termination steps consisting of reaction of phenylnitrene and phenyl azide to afford (E)-azobenzene, the known reaction product of irradiated phenyl azide<sup>11</sup> (eq 3), and/or dimerization of two phenylnitrenes to afford (E)-azobenzene (eq 4), which occurs in dilute solutions.<sup>11</sup> In addition, it is known that molecular oxygen reacts with phenylnitrene<sup>11,12</sup> to form nitrosobenzene as the only primary reaction product,<sup>11</sup> although other products can be observed upon continued

irradiation. The presence of molecular oxygen in solution decreases the measured  $\phi(-\text{PhN}_3)$  value at a given  $[\text{PhN}_3]$ .<sup>7</sup> Quantum yields of disappearance of phenyl isocyanate also exceed unit efficiency at high phenyl isocyanate concentrations.<sup>13</sup>



In order to have a greater understanding of the photoinitiated autocatalytic (branching) chain decomposition of phenyl azide, we have (i) extended our  $\phi(-\text{PhN}_3)$  data<sup>7,8</sup> to include values determined at high  $[\text{PhN}_3]$  in both oxygen-purged and oxygen-saturated solutions and (ii) made a detailed kinetic analysis of the autocatalytic chain decomposition mechanism based upon the experimental variables.

## Experimental Section

**Materials.** Phenyl azide was prepared according to the procedure of Lindsay and Allen<sup>14</sup> by reaction of phenyl hydrazine (Eastman) with nitrous acid, prepared in situ from sodium nitrite (Baker), purified by column chromatography or by vacuum distillation, and characterized by IR, NMR, UV-vis, and mass spectroscopies. 3-Methylpentane (99.4%, Phillips Petroleum) was distilled from Dri-Na (Baker) prior to use. Acetonitrile (Spectrograde, Burdick and Jackson) and prepurified argon, nitrogen, and oxygen gases (West Penn Laco) were used as received. All other chemicals were purchased as reagent grade from either Baker, Eastman, or Fisher and were used as received.

**Instrumentation.** Electronic absorption spectra were recorded on either a Perkin-Elmer Model 330 or Perkin-Elmer Model 575 UV-vis spectrophotometer at room temperature in matched quartz cuvettes (Precision Cells) with pure solvent as the reference. Vibrational absorption spectra were recorded on a Perkin-Elmer Model 580 IR spectrophotometer interfaced to an Interdata 6/16 computer. <sup>1</sup>H nuclear magnetic resonance spectra were recorded on a Hitachi Perkin-Elmer R-24B 60-MHz NMR spectrometer. Mass spectra were recorded on a Varian MAT 112 spectrometer (70 eV) equipped with a SS200 Data System and Varian 1400 gas chromatograph (10% SP 2100 stainless steel column, 6 ft  $\times$  1/8 in.). High-pressure liquid chromatographic (LC) analyses were performed on a Waters ALC/GPC 204 LC and Spectra-Physics Minigrator. A Waters  $\mu$ -porasil column (12  $\times$  1/4 in.), 2% anhydrous diethyl ether in hexane, 1-2 mL/min, and 254- or 280-nm absorbance detection were

\* Address correspondence to this author at the Goodyear Tire and Rubber Company, 142 Goodyear Blvd., Akron, OH 44316.

(1) Reiser, A.; Fraser, V. *Nature (London)* **1965**, 208, 682.

(2) Reiser, A.; Wagner, H. M.; Marley, R.; Bowes, G. *Trans. Faraday Soc.* **1967**, 63, 2423.

(3) Smirnov, V. A.; Brichkin, S. B. *Chem. Phys. Lett.* **1982**, 87, 548.

(4) Reiser, A.; Bowes, G.; Horne, R. J. *Trans. Faraday Soc.* **1966**, 62, 3162.

(5) Reiser, A.; Wagner, H. M.; Bowes, G. *Tetrahedron Lett.* **1966**, 2635.

(6) Reiser, A.; Marley, R. *Trans. Faraday Soc.* **1968**, 64, 1806.

(7) Waddell, W. H.; Lee Go, C. J. *Am. Chem. Soc.* **1982**, 104, 5804.

(8) Lee Go, C. H.; Waddell, W. H. *J. Am. Chem. Soc.* **1984**, 106, 715.

(9) For a review, see: Dainton, F. S. "Chain Reactions. An Introduction"; Wiley: New York, 1966; p 137.

(10) Feilchenfeld, N. B.; Waddell, W. H. *Chem. Phys. Lett.* **1983**, 98, 190.

(11) Lee Go, C.; Waddell, W. H. *J. Org. Chem.* **1983**, 48, 2897.

(12) Abramovitch, R. A.; Challand, S. R. *J. Chem. Soc., Chem. Commun.* **1972**, 964.

(13) Waddell, W. H.; Feilchenfeld, N. B. *J. Am. Chem. Soc.* **1983**, 105, 5499.

(14) Lindsay, R. O.; Allen, C. F. H. "Organic Synthesis"; Wiley: New York, 1955; Collect. Vol. III, p 710.

used. Irradiations were accomplished with use of a Canrad-Hanovia 1000-W Hg-Xe lamp and a Bausch & Lomb High Intensity monochromator, or unfiltered light from a Hanovia 450-W Hg arc.

**Photochemistry.** Quantum yields of disappearance ( $\phi(-\text{PhN}_3)$ ) were determined for ca.  $10^{-1}$  M acetonitrile solutions that were prepared directly and for  $10^{-2}$ – $10^{-5}$  M solutions prepared by volumetric dilution of aliquots of the  $10^{-1}$  M solution. The photochemical reaction was monitored by recording electronic absorption spectral data for each solution prior to and after each irradiation. Absorbances of solutions of  $10^{-4}$  and  $10^{-5}$  M were measured directly and those of higher concentration after volumetric dilution.  $\phi(\text{PhN}_3)$  was calculated from eq 5, where  $N_0 =$

$$\phi(\text{PhN}_3) = \frac{N_0 C V \Delta}{I_0 F t} \quad (5)$$

Avogadro's number in molecules/mmol,  $C$  = concentration in mmol/mL,  $V$  = volume of irradiated solution in mL,  $\Delta$  = fraction of molecules decomposed =  $(A_0 - A_t)/A_0$  where  $A_0$  = absorbance at time = 0 and  $A_t$  = absorbance at time =  $t$ ,  $I_0$  = light intensity measured by irradiating a 0.006 M solution of potassium ferrioxalate,<sup>15</sup>  $F = 1 - 10^{-A_0}$  = the fraction of light absorbed at the irradiating wavelength, and  $t$  = irradiation time in seconds. For  $\phi(-\text{PhN}_3)$  determinations, the fraction of molecules converted was generally less than 3% so that absorption of light by the photoproduct (*(E)*-azobenzene) was negligible.  $\phi(-\text{PhN}_3)$  was measured while an isobestic point was maintained.<sup>8</sup> Actinometry was performed prior to and after sample irradiations in matching cuvettes.

Unless otherwise stated, samples were deoxygenated by bubbling with prepurified nitrogen gas for three minutes at 0 °C and were oxygen-saturated by bubbling with purified oxygen gas for 3 min at 0 °C.

All sample preparations and purifications and photochemical experimentation were performed under red illumination.

## Results and Discussion

Quantum yields of disappearance of phenyl azide ( $\phi(-\text{PhN}_3)$ ) were determined at room temperature for aerated, oxygen-purged, and oxygen-saturated solutions of phenyl azide in acetonitrile. Phenyl azide concentrations ( $[\text{PhN}_3]$ ) of  $1.40 \times 10^{-5}$  to  $7.93 \times 10^{-1}$  M were studied by measuring the decrease in intensity of the 250-nm band maximum of phenyl azide's electronic absorption spectrum upon irradiation with 254-nm light.<sup>8</sup> In general it was observed that for  $[\text{PhN}_3] < 1.3 \times 10^{-4}$  M  $\phi(-\text{PhN}_3)$  values were less than unity:  $\phi(-\text{PhN}_3) = 0.58$ . It was observed that  $\phi(-\text{PhN}_3)$  was not dependent upon whether the solution was oxygen purged vs. oxygen saturated (Table I). Since oxygen is known to quench the photoinitiated autocatalytic chain decomposition (PACD) of phenyl azide<sup>7</sup> but had no effect upon  $\phi(-\text{PhN}_3)$  for  $[\text{PhN}_3] < \text{ca. } 10^{-4}$  M, a chain decomposition reaction is not occurring in these dilute acetonitrile solutions.

For  $\phi(-\text{PhN}_3) \geq 1.60 \times 10^{-4}$  M,  $\phi(-\text{PhN}_3)$  values exceeded unit efficiency. Furthermore,  $\phi(-\text{PhN}_3)$  increased dramatically with increasing  $[\text{PhN}_3]$ . The increase in  $\phi(-\text{PhN}_3)$  appeared to follow an exponential relationship to  $[\text{PhN}_3]$ , but data contained considerable scatter from a simple exponential function for  $[\text{PhN}_3] > 10^{-1}$  M.<sup>8</sup> Since these solutions were air saturated and oxygen is known to quench the PACD reaction,<sup>7</sup>  $\phi(-\text{PhN}_3)$  values were determined for deoxygenated (Table II) and oxygen-saturated (Table III) solutions of phenyl azide with a concentration range of four orders of magnitude (Tables I–III). In order to understand the photoinitiated autocatalytic chain decomposition reaction of phenyl azide, via an exact correlation of  $\phi(-\text{PhN}_3)$  with  $[\text{PhN}_3]$ , a kinetic analysis based upon the proposed reaction mechanism was made for all  $\phi(-\text{PhN}_3)$  data.

The 13-step autocatalytic branching chain decomposition mechanism previously presented<sup>8</sup> can be simplified to 4 steps, eq 1–4, since (i) the kinetic scheme does not differentiate between those reactions of phenylnitrene and phenyl azide which afford a second intermediate (X) which then decomposes into two phenylnitrenes and the direct formation of two phenylnitrenes (eq 2) and (ii) a second reaction intermediate has not yet been observed.<sup>10,13</sup> Thus, the expression for the loss of phenyl azide is given by eq 6, where  $\phi_1$  = quantum yield of reaction 1 (unitless),

$$-\frac{d[\text{PhN}_3]}{dt} = I\phi_1 + k_2[\text{PhN}][\text{PhN}_3] + k_3[\text{PhN}][\text{PhN}_3] \quad (6)$$

**Table I.** Quantum Yields of Disappearance of Phenyl Azide Data for Dilute Acetonitrile Solutions

concn, M	$\phi(-\text{PhN}_3)$
Deoxygenated <sup>a</sup>	
$1.34 \times 10^{-4}$	0.70
$1.29 \times 10^{-4}$	0.97
$2.30 \times 10^{-5}$	0.56
$2.30 \times 10^{-5}$	0.46
$2.13 \times 10^{-5}$	0.66
$1.60 \times 10^{-5}$	0.47
$1.57 \times 10^{-5}$	0.42
$1.40 \times 10^{-5}$	0.31
mean 0.57 (0.19) <sup>b</sup>	
Oxygen Saturated	
$3.25 \times 10^{-4}$	0.75
$1.31 \times 10^{-4}$	0.67
$1.30 \times 10^{-4}$	0.45
$1.26 \times 10^{-4}$	0.38
$3.81 \times 10^{-5}$	0.67
$3.25 \times 10^{-5}$	0.86
$2.53 \times 10^{-5}$	0.41
$2.25 \times 10^{-5}$	0.58
mean 0.59 (0.16) <sup>b</sup>	
overall mean 0.58 (0.19) <sup>b</sup>	

<sup>a</sup> Deoxygenated by bubbling with  $\text{N}_2$  gas. <sup>b</sup> Standard deviation.

**Table II.** Quantum Yields of Disappearance of Phenyl Azide Data in Deoxygenated Acetonitrile at a Constant Photon Flux<sup>a</sup>

concn, M	$\phi(-\text{PhN}_3)$	concn, M	$\phi(-\text{PhN}_3)$
$7.22 \times 10^{-1}$	$1.53 \times 10^4$	$2.76 \times 10^{-2}$	$2.94 \times 10^2$
$6.14 \times 10^{-1}$	$1.29 \times 10^4$	$5.24 \times 10^{-3}$	$4.04 \times 10^1$
$1.29 \times 10^{-1}$	$3.58 \times 10^3$	$4.15 \times 10^{-3}$	$5.23 \times 10^1$
$7.73 \times 10^{-2}$	$6.79 \times 10^2$	$3.21 \times 10^{-3}$	$1.59 \times 10^1$
$5.65 \times 10^{-2}$	$5.63 \times 10^2$	$3.96 \times 10^{-4}$	1.59

<sup>a</sup>  $I_0 = 5.46 \times 10^{14}$  photons/s.

**Table III.** Quantum Yield of Disappearance of Phenyl Azide Data in Oxygen-Saturated Acetonitrile at a Constant Photon Flux<sup>a</sup>

concn, M	$\phi(-\text{PhN}_3)$	concn, M	$\phi(-\text{PhN}_3)$
$7.93 \times 10^{-1}$	$2.28 \times 10^3$	$3.83 \times 10^{-2}$	$4.92 \times 10^1$
$2.40 \times 10^{-1}$	$4.55 \times 10^2$	$3.61 \times 10^{-3}$	$1.33 \times 10^1$
$1.76 \times 10^{-1}$	$4.14 \times 10^2$	$2.68 \times 10^{-3}$	1.06
$6.32 \times 10^{-2}$	$5.30 \times 10^1$	$1.73 \times 10^{-3}$	7.15
$5.73 \times 10^{-2}$	$8.21 \times 10^1$		

<sup>a</sup>  $I_0 = 5.46 \times 10^{14}$  photons/s.

$I$  = intensity of absorbed light ( $\text{einstein} \cdot \text{L}^{-1} \cdot \text{s}^{-1}$ ),  $k_2$  = rate constant of reaction 2, and  $k_3$  = rate constant of reaction 3.

A steady-state assumption is made for  $[\text{PhN}]$  which affords a quadratic equation which when solved exactly and substituted into eq 6 yields eq 7. It can be seen from eq 7 that if  $I$  is a

$$-\frac{d[\text{PhN}_3]}{dt} = I\phi_1 + [(k_2 + k_3)(k_2 - k_3)/4k_4][\text{PhN}_3]^2 + [(k_2 + k_3) \times (k_2 - k_3)/4k_4]^2[\text{PhN}_3]^4 + ((k_2 + k_3)^2\phi_1/2k_4)I[\text{PhN}_3]^2]^{1/2} \quad (7)$$

constant and the percent conversion is low so that  $[\text{PhN}_3]$  is a virtual constant then  $-d[\text{PhN}_3]/dt$  is a constant with time, which has been experimentally verified.<sup>8,11</sup> Thus,

$$\frac{-d[\text{PhN}_3]}{dt} = -\frac{\Delta[\text{PhN}_3]}{\Delta t} \quad (8)$$

and by definition

$$\phi(-\text{PhN}_3) = -\frac{\Delta[\text{PhN}_3]}{\Delta t} \frac{1}{I} \quad (9)$$

where  $\Delta[\text{PhN}_3]$  has the units of M and will be negative (thus affording a positive  $\phi(-\text{PhN}_3)$  value) and  $\Delta t$  has the units of s.

**Table IV.** Quantum Yield of Disappearance of Phenyl Azide Data in Deoxygenated Acetonitrile<sup>a</sup>

concn, M	$\phi(-\text{PhN}_3)$	$I_0$ , photons/s
$3.00 \times 10^{-2}$	$3.00 \times 10^2$	$4.00 \times 10^{14}$
$3.00 \times 10^{-3}$	$5.25 \times 10^1$	$4.00 \times 10^{14}$
$3.00 \times 10^{-4}$	3.49	$4.00 \times 10^{14}$
$2.30 \times 10^{-4}$	2.11	$1.18 \times 10^{14}$
$1.60 \times 10^{-4}$	1.83	$1.53 \times 10^{14}$
$1.60 \times 10^{-4}$	1.57	$6.48 \times 10^{14}$

<sup>a</sup>Deoxygenated by N<sub>2</sub> bubbling.

Combining eq 7–9 affords eq 10, since the negative solution can be neglected when  $\phi(-\text{PhN}_3) \geq \phi_1$ , which is always the case.

$$\phi(-\text{PhN}_3) = \phi_1 + [(k_2 + k_3)(k_2 - k_3)/4k_4][\text{PhN}_3]^2/I + [((k_2 + k_3)(k_2 - k_3)/4k_4)^2[\text{PhN}_3]^2/I^2 + ((k_2 + k_3)^2\phi_1/2k_4)[\text{PhN}_3]^2/I]^{1/2} \quad (10)$$

As  $[\text{PhN}_3]$  becomes more dilute, the term  $[\text{PhN}_3]^2/I$  will become increasingly smaller and  $\phi(-\text{PhN}_3)$  will approach the constant value of  $\phi_1$ . Alternatively, when  $[\text{PhN}_3]^2/I$  is sufficiently large, the term  $[(k_2 + k_3)^2\phi_1/2k_4][\text{PhN}_3]^2/I$  becomes negligible and eq 11 can be obtained if  $I$  is expanded, where  $N_0$  = Avogadro's

$$\phi(-\text{PhN}_3) = \phi_1 + 2[(k_2 + k_3)(k_2 - k_3)/4k_4]N_0 \frac{[\text{PhN}_3]^2 V_0}{I_0(1 - 10^{-A_0})} \quad (11)$$

number,  $I_0$  = light intensity measured by ferrioxalate actinometry,<sup>15</sup>  $A_0$  = absorbance at time = 0, and  $V_0$  = volume of irradiated solution in L. When  $[\text{PhN}_3]^2/I$  is large the constraint  $\phi(-\text{PhN}_3) \gg \phi_1$  can be applied to obtain eq 12. Since  $[\text{PhN}_3]$ ,  $V_0$ ,  $I_0$ , and  $\log \phi(-\text{PhN}_3) = \log 2[(k_2 + k_3)(k_2 - k_3)/4k_4]N_0 + \log [[\text{PhN}_3]^2 V_0 / I_0(1 - 10^{-A_0})] \quad (12)$

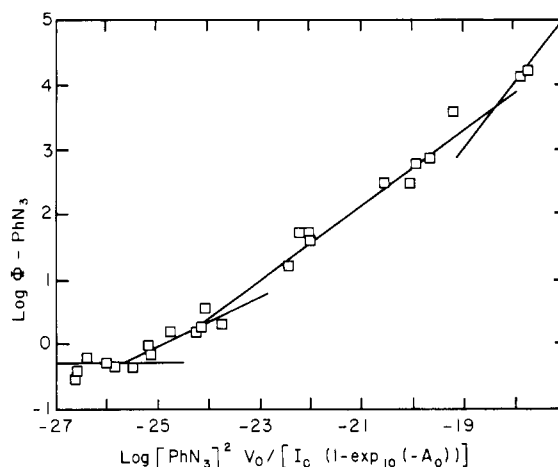
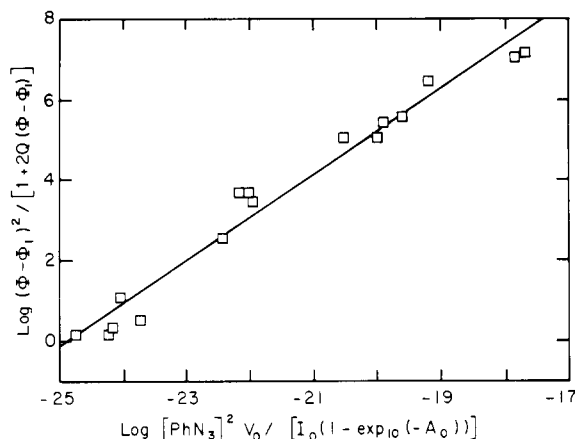
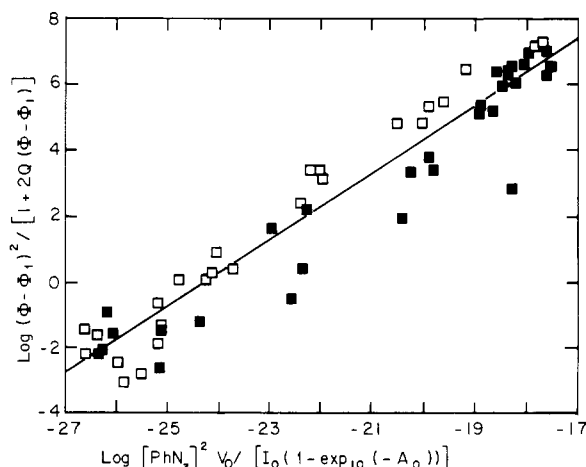
$A_0$  are experimental variables, plots of  $\log \phi(-\text{PhN}_3)$  vs.  $\log [[\text{PhN}_3]^2 V_0 / I_0(1 - 10^{-A_0})]$  should be linear having a slope of 1.0 and an intercept of  $\log (2N_0(k_2 + k_3)(k_2 - k_3)/4k_4)$ . Thus, a plot of  $\log \phi(-\text{PhN}_3)$  vs.  $\log [[\text{PhN}_3]^2 V_0 / I_0(1 - 10^{-A_0})]$  for  $\phi(-\text{PhN}_3)$  data determined over the four order-of-magnitude  $[\text{PhN}_3]$  range should display a curve where the slope is changing from zero to one as  $[\text{PhN}_3]$  approaches very large values. Such behavior is observed (Figure 1) for all  $\phi(-\text{PhN}_3)$  data determined in deoxygenated solution (Tables I, II, and IV) since the slope of this plot is approaching, but has not yet reached, a value of unity. It should be noted that for the highest  $[\text{PhN}_3]$  examined, the limiting case of eq 12 has not yet been reached, thus the more general eq 10 must be applied to the  $\phi(-\text{PhN}_3)$  data analysis.

Equation 13 can be obtained from eq 10 without making any assumptions where  $Q = (k_2 - k_3)/[2\phi_1(k_2 + k_3)]$ . Since  $\phi \approx 0.5$  (Table I),  $Q(k_2 - k_3)/(k_2 + k_3) \leq 1.0$ . Equation 13 applies

$$\log [(\phi(-\text{PhN}_3) - \phi_1)^2 / (1 + 2Q(\phi(-\text{PhN}_3) - \phi_1))] = \log [(k_2 + k_3)^2 \phi_1 N_0 / 2k_4] + \log [[\text{PhN}_3]^2 V_0 / (I_0(1 - 10^{-A_0}))] \quad (13)$$

exactly to all  $\phi(-\text{PhN}_3)$  values determined in deoxygenated solution (Table I, II, and IV), thus a plot of  $\log [(\phi(-\text{PhN}_3) - \phi_1)^2 / (1 + 2Q(\phi(-\text{PhN}_3) - \phi_1))]$  vs.  $\log [[\text{PhN}_3]^2 V_0 / (I_0(1 - 10^{-A_0}))]$  should be linear with a slope of exactly 1.00. Note that all variables are experimentally determined values with the exception of  $Q$ . While there is no way to estimate  $Q$ , limits can be extended to it: (i)  $Q \leq 1.0$  since  $Q \approx (k_2 - k_3)/(k_2 + k_3)$  and (ii)  $Q > -1/2\phi(-\text{PhN}_3)$  or the entire expression would be negative. Such behavior of  $\phi(-\text{PhN}_3)$  is verified as shown in Figure 2 for the  $\phi(-\text{PhN}_3)$  values determined in deoxygenated acetonitrile (Tables II and IV) which affords a slope of 1.00 and  $r^2$  (correlation coefficient for the least-squares linear fit of the data) of 0.969 when  $Q = 0.0019$ .

A similar analysis was made for all available  $\phi(-\text{PhN}_3)$  data whether deoxygenated oxygen, saturated (Table III), or air sat-

**Figure 1.** Plot of  $\log \phi(-\text{PhN}_3)$  vs.  $\log [[\text{PhN}_3]^2 V_0 / I_0(1 - 10^{-A_0})]$  for  $\phi(-\text{PhN}_3)$  values obtained in deoxygenated acetonitrile (Tables I, II, and IV).**Figure 2.** Plot of  $\log [(\phi - \phi_1)^2 / (1 + 2Q(\phi - \phi_1))]$  vs.  $\log [[\text{PhN}_3]^2 V_0 / I_0(1 - 10^{-A_0})]$  for  $\phi(-\text{PhN}_3)$  values obtained in deoxygenated acetonitrile (Tables II and IV), where  $\phi = \phi(-\text{PhN}_3)$ ,  $\phi_1 = 0.58$  (Table I),  $Q = 0.0019$ , and  $r^2 = 0.969$ .**Figure 3.** Plot of  $\log [(\phi - \phi_1)^2 / (1 + 2Q(\phi - \phi_1))]$  vs.  $\log [[\text{PhN}_3]^2 V_0 / I_0(1 - 10^{-A_0})]$  for  $\phi(-\text{PhN}_3)$  values obtained in deoxygenated (□, Tables I, II, and IV) and oxygen-saturated and air-saturated (●, Tables I, III, and IV) acetonitrile, where  $\phi = \phi(-\text{PhN}_3)$ ,  $\phi_1 = 0.58$  (Table I),  $Q = 0.0004$ , and  $r^2 = 0.852$ .

urated (Table IV) (Figure 3). A slope of 1.02 is obtained for the best least-squares fit of the data ( $r^2 = 0.852$ ) with  $Q = 0.0004$ . Figure 3 also shows data from Table I although a PACD reaction is not thought occurring in these dilute solutions.

The very small values of  $Q$  which afford good fits of the data

**Table V.** Quantum Yield of Disappearance of Phenyl Azide Data in Air-Saturated Acetonitrile Solutions<sup>a</sup>

concn, M	$\phi(-\text{PhN}_3)$	$I_0$ , photons/s	$V_0$ , mL
$3.79 \times 10^{-1}$	$2.71 \times 10^1$	$1.11 \times 10^{15}$	4.0
$2.18 \times 10^{-1}$	$2.60 \times 10^3$	$4.02 \times 10^{14}$	3.5
$2.02 \times 10^{-1}$	$9.11 \times 10^3$	$7.28 \times 10^{13}$	4.0
$1.95 \times 10^{-1}$	$3.78 \times 10^3$	$2.74 \times 10^{14}$	3.5
$1.84 \times 10^{-1}$	$3.34 \times 10^3$	$2.42 \times 10^{14}$	3.5
$1.74 \times 10^{-1}$	$3.78 \times 10^3$	$3.70 \times 10^{13}$	3.5
$1.69 \times 10^{-1}$	$8.82 \times 10^3$	$1.11 \times 10^{14}$	4.0
$1.69 \times 10^{-1}$	$1.62 \times 10^3$	$1.87 \times 10^{14}$	4.0
$1.64 \times 10^{-1}$	$2.89 \times 10^3$	$2.79 \times 10^{14}$	3.5
$1.58 \times 10^{-1}$	$1.42 \times 10^3$	$2.64 \times 10^{14}$	3.5
$1.37 \times 10^{-1}$	$4.33 \times 10^3$	$7.64 \times 10^{13}$	3.5
$1.25 \times 10^{-1}$	$2.92 \times 10^3$	$2.48 \times 10^{14}$	4.0
$8.68 \times 10^{-2}$	$6.03 \times 10^2$	$2.48 \times 10^{14}$	4.0
$3.25 \times 10^{-2}$	9.96	$1.07 \times 10^{15}$	4.0
$3.25 \times 10^{-3}$	2.10	$9.89 \times 10^{14}$	4.0

<sup>a</sup>  $A_0 > 3.0$ .

shown in Figures 2 and 3 indicate that  $k_2$  and  $k_3$  are essentially equal. Since both reactions 2 and 3 depend upon a phenylnitrene/phenyl azide interaction, that  $k_2 \approx k_3$  is not unexpected. If  $k_2 \approx k_3$ , then from the value of the intercept in Figure 2 (24.84) eq 13 yields the relationship  $k_2 \approx (0.1k_4)^{1/2}$ ; however, in view of the length of the required extrapolation, this value provides only a rough estimate.

Equation 10 also predicts that if  $[\text{PhN}_3]$  and  $V_0$  are constants,  $\phi(-\text{PhN}_3)$  will depend upon  $I_0$  such that as  $I_0$  is increased,  $\phi(-\text{PhN}_3)$  should decrease. While only limited data are available the decrease in  $\phi(-\text{PhN}_3)$  with increasing  $I_0$  is evident from data at  $[\text{PhN}_3] = 1.60 \times 10^{-4}$  M (Table IV) and  $[\text{PhN}_3] = 1.69 \times 10^{-1}$  M (Table V). This relationship is quite notable for the latter case since an increase in  $I_0$  from  $1.11 \times 10^{14}$  to  $1.87 \times 10^{14}$  photons/s results in a decrease in  $\phi(-\text{PhN}_3)$  from  $8.82 \times 10^3$  to  $1.62 \times 10^3$ . Also notable is the unusually low  $\phi(-\text{PhN}_3)$  value of  $2.71 \times 10^1$  determined at  $[\text{PhN}_3] = 3.79 \times 10^{-1}$  and  $I_0 = 1.11$

$\times 10^{15}$ , the highest value of  $I_0$  utilized in these experiments (Table V).

One measure of the validity of this kinetic treatment of the experimental results is its ability to predict the experimental parameters based upon the simplified four-step reaction mechanism. Indeed, eq 10 correlates (i) all  $\phi(-\text{PhN}_3)$  values ranging from 0.3 to 15000, (ii) all  $[\text{PhN}_3]$  data ranging from  $1.40 \times 10^{-5}$  to  $7.93 \times 10^{-1}$  M, (iii) all  $\phi(-\text{PhN}_3)$  data whether determined in oxygen-purged, oxygen-saturated, or air-saturated solution, and (iv) the variation of  $\phi(-\text{PhN}_3)$  with  $I_0$ .

Finally, eq 10 and Figures 1-3 serve to clarify the photoinitiated autocatalytic (branching) chain decomposition (PACD) reaction of phenyl azide in solution, hence further documentation of the *first molecular explosion in solution*.<sup>8</sup>

## Conclusion

Upon irradiation of phenyl azide in dilute acetonitrile solution, molecular nitrogen is lost<sup>4-6</sup> and phenylnitrene is formed.<sup>1-3</sup>  $\phi(-\text{PhN}_3) = 0.58$  for  $[\text{PhN}_3] < 10^{-4}$  M. Dimerization of two phenylnitrenes leads to (*E*)-azobenzene formation.<sup>11</sup> At higher  $[\text{PhN}_3]$  phenylnitrene reacts with phenyl azide to afford two phenylnitrenes,<sup>10,13</sup> which then react further. This autocatalytic branching chain decomposition reaction<sup>9</sup> is manifested as  $\phi(-\text{PhN}_3)$  values that greatly exceed unit efficiency.<sup>7,8</sup> A kinetic analysis of a simplified four-step reaction mechanism provides a mathematical expression that serves to explain the variation of  $\phi(-\text{PhN}_3)$  with  $[\text{PhN}_3]$ ,  $I_0$ , and  $V_0$ .  $\phi(-\text{PhN}_3)$  increases with increasing  $[\text{PhN}_3]$ <sup>2</sup> and decreases with increasing  $I_0$ . The mathematical expression fitting the 56 experimental determinations of  $\phi(-\text{PhN}_3)$  affords further definitive evidence of the *first molecular explosion in solution*.<sup>8</sup>

**Acknowledgment.** We wish to thank the National Science Foundation for support of this research via a grant to the Center for the Joining of Materials (DMR 76-81561).

**Registry No.** Phenyl azide, 622-37-7.

## Molecular Structure as Reflected in the <sup>13</sup>C NMR Spectra of Oligosaccharides with Partially Deuterated Hydroxyls<sup>1</sup>

Jacques Reuben

Contribution No. 1803 from Hercules Incorporated, Research Center, Wilmington, Delaware 19894. Received June 27, 1984

**Abstract:** This paper presents a new approach to the <sup>13</sup>C NMR analysis of oligosaccharides. The approach is based on the recently described structural effects on the isotopic multiplets in the spectra of materials with partially deuterated hydroxyls and on some well-known features of the <sup>13</sup>C chemical shifts of carbohydrates. It is shown that the kind and number of isotopic multiplets for the nonanomeric methines (carbons 2, 3, 4, and 5 of aldohexoses, carbons 3, 4, and 5 of ketohexoses) form sets characteristic of the position of substitution and can be used in tracking the sequence of glycosidic linkages. In favorable cases, ab initio analysis of di- and trisaccharides is possible by this approach. As examples, the isotopic multiplets in the spectra of  $\alpha$ -lactose and a series of fructose-containing oligosaccharides are examined in detail.

Carbon-13 NMR spectroscopy has taken a prominent place beside the traditional chemical and enzymological approaches to the structure elucidation of complex carbohydrates. The use of <sup>13</sup>C chemical shifts in structural studies of oligosaccharides in solution requires comparison with the spectra of monosaccharides and knowledge of empirical rules governing substituent effects.<sup>2,3</sup> The application of such approaches is based on known monosaccharide composition and resonance assignments. Several as-

signment techniques of increasing complexity are available.<sup>2-4</sup> The most elaborate among them is two-dimensional NMR, which relies only on some well-established facts regarding the chemical shifts of the anomeric carbons and hydrogens.<sup>4</sup> Unequivocal spectral assignments can also be obtained from the isotopic multiplets in the spectra of carbohydrates with partially deuterated hydroxyls (in Me<sub>2</sub>SO solutions).<sup>5,6</sup> These multiplets are due to small upfield deuterium isotope effects on <sup>13</sup>C chemical shifts: 0.09–0.12 ppm for directly bonded hydroxyls ( $\Delta_\beta$ ) and 0.07 ppm or less for

(1) Part 4 in the series: "Isotopic Multiplets in the <sup>13</sup>C NMR Spectra of Polyols with Partially Deuterated Hydroxyls". For part 3 see: Reuben, J. J. *Am. Chem. Soc.* **1984**, *106*, 6180-6186.

(2) Gorin, P. A. J. *Adv. Carbohydr. Chem. Biochem.* **1981**, *38*, 13-104.

(3) Bock, K.; Petersen, C. *Adv. Carbohydr. Chem. Biochem.* **1983**, *41*, 27-66.

(4) Morris, G. A.; Hall, L. D. *J. Am. Chem. Soc.* **1981**, *103*, 4703-4711, and references therein.

(5) Reuben, J. J. *Am. Chem. Soc.* **1983**, *105*, 3711-3713.

(6) Christofides, J. C.; Davies, D. B. *J. Am. Chem. Soc.* **1983**, *105*, 5099-5105; *J. Chem. Soc., Chem. Commun.* **1983**, 324-326.